


 Cite this: *RSC Adv.*, 2022, 12, 13756

Improving the curing and flame retardancy of epoxy resin composites by multifunctional Si-containing cyclophosphazene derivatives

 Wang-Xi Fan,^a Zefang Li,^b Zhou Yang,^a Jun-Fei Ou,^a Meng Xiang^a and Zhong-Li Qin^{*c}

Novel star-like molecules containing P, N and Si with dual functions of flame retardance and curing promotion (abridged as HCCP–KH540) were successfully synthesized through the nucleophilic substitution reaction of hexachlorocyclotriphosphazene (HCCP) and 3-aminopropyltrimethoxysilane (KH540). HCCP–KH540 was incorporated with the matrix of epoxy resin (EP) to form a flame retardant composite abridged as E–HK. The activation energy of the curing reaction of the E–HK composite was reduced but the curing reaction rate was accelerated by HCCP–KH540. The E–HK composite with 30 phr content of HCCP–KH540 exhibited excellent flame retardancy with limiting oxygen index of 29.6% and V-1 rating in the vertical burning test as well as excellent thermal stability with a char yield of 23.77% at 700 °C, compared with only 8.64% for pure EP.

 Received 5th December 2021
 Accepted 7th April 2022

DOI: 10.1039/d1ra08843b

rsc.li/rsc-advances

Introduction

As one class of important thermoset polymers, epoxy (EP) resins are widely applied in high-performance composites, such as in the aerospace, military, marine, and automobile industries due to excellent thermal stability, and high cohesiveness but low shrinkage.^{1–3} The requirements of multi-functionalization and highly efficient manufacturing for modern intelligent products are increasing. Therefore, it is urgent to endow EP resins simultaneously with flame retardancy, low curing temperature and high curing rate.^{4–7}

Various additives, such as halogen compounds,⁸ and aluminium based,^{9,10} nitrogen based¹¹ and phosphorus based flame retardants,⁷ can be used to improve the flame retardancy of epoxy resins. However, they all show certain limitations. For example, additives are easy to precipitate from the EP resin matrix due to compatibility between additives and EP resins. The mechanical properties of the EP resin are reduced due to the addition of a large amount of flame retardant.^{8–10} Even some additives, such as halogen compounds, potentially release corrosive and toxic chemicals during combustion, which easily causes secondary injury to people.⁸ Fortunately, bulk flame retardant products are prepared by introducing flame retardant groups into the molecular chain of EP resin, which can overcome these shortcomings. Therefore, hexachlorocyclotriphosphazene (HCCP) has gradually attracted

people's attention because of its strong flame retardancy and high reactivity.^{12–16}

The molecular structure of HCCP contains Cl, P and N elements simultaneously, which can form a P–N synergistic flame retardant system resulting in excellent flame retardant properties. Therefore, HCCP can be used in fire retardant materials and self extinguishing materials.^{12–14} However, HCCP used as a flame retardant directly is prone to secondary pollution due to HCl produced by combustion. Functionalization HCCP can be easily obtained by nucleophilic substitution of Cl atoms bonded to phosphorus with a nucleophile including amine, alcohol, or water. Therefore, derivatives of HCCP with dual or multi-function and good compatibility with the polymer matrix have been widely concerned.^{15,16} For example, Huang and *et al.* prepared a novel anti-aging flame retardant through the nucleophilic substitution reaction of 4,4'-biphenol and HCCP.¹⁴ Ning *et al.* Synthesized a new cyclotriphosphazene derivative with high flame retardant efficiency and smoke suppression performance by using a thiazole with simple chemical structure to react with cyclotriphosphazene.¹⁵

In addition, the application range of EP resin is limited due to the increased brittleness and reduced toughness caused by the extensive use of curing agent.^{17,18} Therefore, on the premise of meeting the application performance, the amount of curing agent should be reduced as far as possible.

Functional groups are introduced into the ring structure of HCCP by utilizing the high reactivity of HCCP, which can not only reflect the crosslinking and curing effect of secondary amine on EP, but also realize the synergistic flame retardant effect of P–N. In this article, a new HCCP derivative (HCCP–KH540) with a star-like network structure was successfully

^aSchool of Materials Engineering, Jiangsu University of Technology, Changzhou, China

^bSchool of Computer Engineering, Jiangsu University of Technology, Changzhou, China

^cSchool of Electronics and Information Engineering, Hubei University of Science and Technology, Xianning, China. E-mail: qinzhongli@hbust.edu.cn


prepared by introducing Si-containing functional groups into HCCP. Furthermore, HCCP-KH540 was added in epoxy matrix as an additive with dual functions of flame retardant and curing promotion to prepare a composite (E-HK) with excellent curing and flame retardancy. The effects of HCCP-KH540 on curing, thermal property and flame retardancy in E-HK were discussed in detail.

Experimental

Materials

HCCP (98%) and epoxy resin (E-51) used in this study was obtained from Aladdin Reagent Co. Ltd, Shanghai, China; KH540 was obtained from Markun Reagent Co., Ltd, Xiamen, China; tetrahydrofuran (THF, A.R.), diethylenetriamine (A.R.) and triethylamine (A.R.) and absolute ethanol was obtained from Shenzhen Linfeng Reagent Co. Ltd, Shenzhen, China.

Synthesis of HCCP-KH540

For a typical experiment, HCCP (6.95 g) was added into a four necked flask containing THF (80 mL) and stirred for 30 minutes at 65 °C under nitrogen atmosphere. A mixed solution of 20.95 mL KH540 and 5 mL triethylamine was added dropwise into the four necked flask within 20 minutes, and the reaction continued for about 7 hours under nitrogen atmosphere after dropwise addition. Subsequently, the solvent THF was removed by vacuum distillation. White products were obtained by washing with *n*-heptane and deionized water for 3 times, followed by drying at 60 °C for 36 hours in a vacuum oven. Synthesis schematic diagram and star-like structure of HCCP-KH540 is shown in Fig. 1a.

Preparation of E-HK composites

Appropriate amounts of curing agent (diethylenetriamine) and epoxy resins (E-51) were added in a double necked flask and were stirred at 60 °C for 15 minutes with a mechanical stirrer. Varying amounts of HCCP-KH540 was poured into the double necked flask and was stirred for 30 minutes. The prepared mixture was poured into some molds with cavity size of 100 mm × 10 mm × 4 mm made of polytetrafluoroethylene and was placed in a vacuum oven at 60 °C for 120 minutes to remove the air bubbles. Then the mixture was cured at 100 °C and 160 °C for 120 minutes, respectively. The composite products were obtained and named as E-HK after cooling, demoulding and edge removal. Amount of HCCP-KH540 in the E-HK composites was 0, 5, 10, 20, and 30 phr, respectively.

Instrumentation

Fourier transform infrared (FT-IR) spectra of KH540 and HCCP-KH540 were recorded on a Nicolet IS10 FT-IR spectrometer, and the samples were scanned at room temperature over a range of wavenumber from 650 to 4000 cm⁻¹, wherein 32 scans were collected during each spectroscopic measurement. The ¹H and ³¹P nuclear magnetic resonance (¹H NMR and ³¹P NMR) spectra of HCCP-KH540 were recorded on a MicroMR12-025V

spectrometer, employing CDCl₃ as solvent. The fracture morphology of the E-HK composites was obtained by Field Emission Scanning Electron Microscope (Sigma 500). Thermal gravimetric (TG) of the E-HK composites was analyzed on a DTA7300 thermal analyzer with appropriate heating rates from 20 °C to 700 °C, operating under a N₂ atmosphere. Limiting oxygen index (LOI) of E-HK specimens was characterized by using a JF-3 oxygen index meter according to GB/T2406-2008. X-ray photoelectron spectroscopy (XPS) and Raman spectra of char residues were recorded on a ThermoFischer ESCALAB Xi+ and Dxr2xi spectrometer, respectively. Combustion properties of EP and E-HK composites were tested by a cone calorimeter model Icone Classic FTT according to ISO-5660-1 standard. The sample is 100 mm × 100 mm × 4 mm and thermal radiation power is 50 kW m⁻², respectively.

Results and discussion

Element and structure analysis

Fig. 1b illustrates typical FT-IR spectra of KH540 and HCCP-KH540 samples. The peaks centered at 2900 cm⁻¹ corresponding to the motions of C-H and the bands centered at 3408 cm⁻¹ and 3371 cm⁻¹ assigned to primary amino are clearly found in HCCP spectrum. For HCCP-KH540, a new vibrational absorption appears at 1027 cm⁻¹ and the wide bands at 3358 cm⁻¹ assigned to secondary amino, which indicates the new P-N bond has been successfully generated.^{19,20}

Fig. 1c and d exhibits the chemical structure of HCCP-KH540 characterized by ¹H NMR and ³¹P NMR spectrum. It can be clearly observed from Fig. 1c that the chemical shifts at 3.50 ppm are assigned to the hydrogen atoms of methoxyl (-OCH₃) and secondary amino (-NH-). The peaks centered at 2.58 and 0.56 ppm can be ascribed to the hydrogen atoms of -CH₂- connected to N (-CH₂-N-) and Si (-Si-CH₂-), respectively. A peak at 1.50 ppm is attributed to hydrogen atoms of -CH₂-, which is the only secondary carbon atom in structure of HCCP-KH540.^{21,22} As evidenced by FT-IR analyses in the previous section, the results of ¹H NMR analysis further prove that HCCP-KH540 was successfully prepared. In Fig. 1d, the only one peak centered at 23.6 ppm is assigned to P atom of HCCP-KH540, which indicates that the chemical environment of P is relatively uniform and the desired reaction takes place.

The morphologies and element analysis of HCCP and HCCP-KH540 are observed by SEM and EDS respectively, which are summarized in Fig. 1d and e. P, N and Cl amounts of HCCP are 42.9%, 18.7% and 30.6% as shown in Fig. 1e. After the reaction of HCCP and KH540, the P, N and Si amounts of produced HCCP-KH540 are 7.4%, 11% and 13.7% as shown in Fig. 1f, respectively, which are close to the theoretical values respectively.

As shown in Fig. 1e, HCCP appeared loose reticular or filamentous structure with vast large pores, which is conducive to chemical reaction with KH540. For the HCCP-KH540 shown in Fig. 1f there are some typical irregular lumps with dimensions of ~300 μm in diameter. HCCP-KH540 was produced efficiently by the nucleophilic substitution reaction of HCCP and KH540, in which the amino group in KH540 molecule lost the H atoms



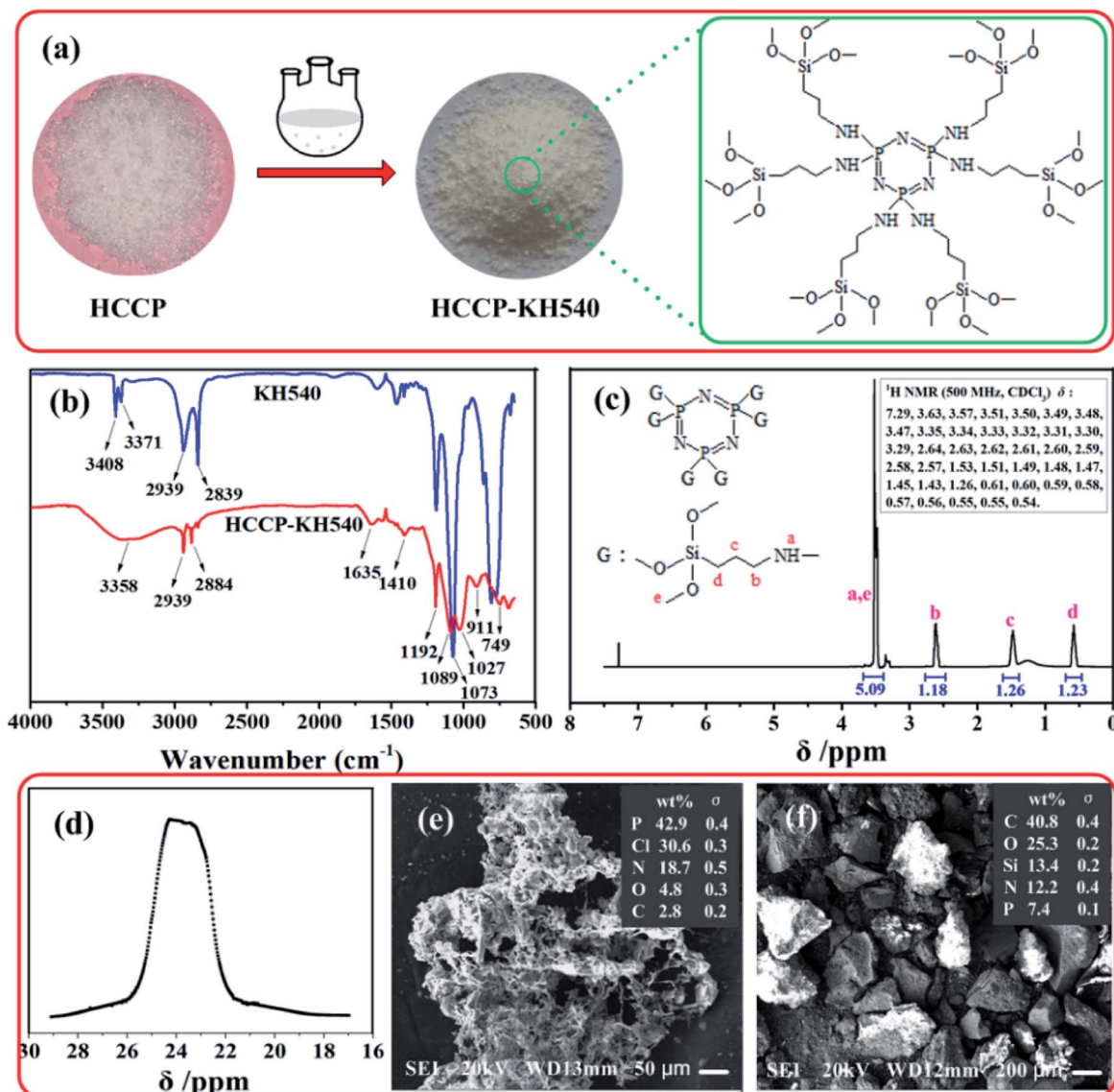


Fig. 1 Synthesis route, element and structure analysis of HCCP-KH540: (a) synthesis route; (b) FTIR of HCCP and HCCP-KH540; (c) ^1H NMR of HCCP-KH540; (d) ^{31}P NMR of HCCP-KH540; (e and f) SEM of HCCP and HCCP-KH540, the inset shows element content measurement result by EDS.

and was linked to aromatic ring by N-P bond,²³ and finally resulted in a bigger size of HCCP-KH540.

Curing kinetics of EP and E-HK composites

HCCP-KH540 has the potential to promote the curing of EP matrix because of the secondary amine in the structure. To evaluate the curing property of HCCP-KH540, two serials of epoxy resin composites (*i.e.* EP and E-HK) were used to test the curing kinetics by non-isothermal DSC method. Dynamic DSC thermograms for the EP and E-HK at different heating rates (β , $\beta = 5, 10, 15$ and $20\text{ }^\circ\text{C min}^{-1}$) under N_2 atmosphere with diethylenetriamine as curing agent are shown in Fig. 2.

It can be clearly observed from Fig. 2a and b that the exothermic peak temperatures of the curing curves of EP and E-HK moved to higher temperature as the heating rate

increases from 5 to $20\text{ }^\circ\text{C min}^{-1}$. As expected, the exothermic peak temperatures of the curing curves of E-HK are higher than those of EP, which indicates that HCCP-KH540 can increase the curing temperature and accelerate the curing rate of E-HK composites. This is further confirmed by the subsequent curing temperature data obtained by extrapolation of $T-\beta$ curve of the EP and E-HK at different β (see Fig. 2c and d).

Ozawa and Kissinger methods^{17,18,24,25} were used to calculate frequency factor (A) and activation energy (E_k) because they were both simple methods to deal with the dynamic curing process of epoxy/amine composites. The kinetic parameters calculated by Ozawa and Kissinger methods do not need any assumption to convert the relevant equations. Kissinger's equation is as following:



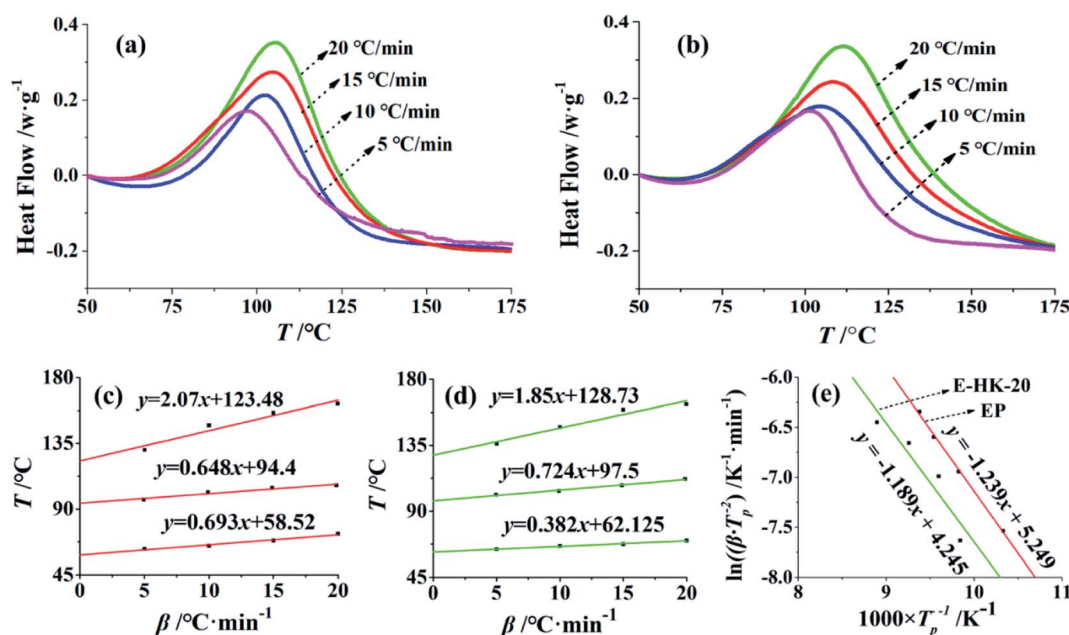


Fig. 2 DSC thermograms of EP (a) and E-HK-20 (b), T - β curve of EP (c) and E-HK-20 (d) at different β under N_2 atmosphere, and $\ln(\beta/T_p^2)-1/T_p$ curve by Kissinger method in different curing reaction (e).

$$\ln\left(\frac{\beta}{T_p^2}\right) = -\frac{E_k}{RT_p} + \ln\frac{AR}{E_k} \quad (1)$$

where R , A is ideal gas constant and Arrhenius constant, respectively. Therefore, E_k of curing reactions of EP and E-HK could be calculated from the slope of $\ln(\beta/T_p^2)$ vs. $1/T_p$ plot (see Fig. 2e). E_k of curing reactions of EP and E-HK composites is summarized in Table 1, respectively. Obviously, E_k of E-HK composites declines from 103 kJ mol^{-1} to 95 kJ mol^{-1} as their HCCP-KH540 contents increase from 0 to 30 phr, which indicates that HCCP-KH540 can reduce the E_k of curing reaction and accelerate the curing reaction rate of E-HK composites.

In order to understand the influence of HCCP-KH540 on the glass transition temperature (T_g), T_g of EP and E-HK composites with different content of HCCP-KH540 measured by DSC method are summarized in Table 1. Due to the increase of the crosslinking degree of EP molecules chain caused by the curing reaction of EP and the secondary amine group in HCCP-KH540, the movement of EP resin molecules chain is blocked and the flexibility is reduced, which eventually leads to the T_g of E-HK composites with different content of HCCP-KH540 increased

from 55.6 °C to 67.3 °C as their HCCP-KH540 contents increase from 0 to 30 phr.

Thermal stability of EP and E-HK composites

TG was used to evaluate the thermal stability of EP and E-HK composites, and the results of TG analysis are summarized in Fig. 3. The initial decomposition temperature ($T_{5\%}$) and maximum decomposition temperature (T_{\max}) of EP resin without flame retardant appear at 366.7 and 389.3 °C, respectively, which are mainly attributed to the degradation reaction of EP molecular chain. Meanwhile, the char yield of the EP is 8.64% at 700 °C, as shown in Fig. 3a. Comparing with the EP resin without flame retardant, the $T_{5\%}$ of E-HK composites declines from 356.48 °C to 259.8 °C, but the char yield increases from 8.88% to 23.77% at 700 °C, respectively, as the amount of HCCP-KH540 increases from 5 to 30 phr. Furthermore, the T_{\max} of E-HK composites declines from 388.9 °C to 383.9 °C, and the weight loss speed of EP and E-HK composites declines from 4792.3 to 1708.1 $\mu\text{g min}^{-1}$, which indicates that HCCP-KH540 can reduce T_{\max} and the decomposition rate of E-HK

Table 1 Composition and flame retardancy data of EP and E-HK

Sample	EP/g	Diethylene-triaminen/phr	$T_g/^\circ\text{C}$	$E_k/(\text{kJ mol}^{-1})$	HCCP-KH540/phr	LOI/%	UL-94	
							Dripping	UL-94 rating
EP	100	15	55.6	103	0	22.4 ± 0.10	Yes	No rating
E-HK-5	100	10	55.9	102	5	25.5 ± 0.09	Yes	No rating
E-HK-10	100	10	56.3	100	10	26.1 ± 0.11	No	No rating
E-HK-20	100	10	59.4	98	20	27.1 ± 0.10	No	V-2
E-HK-30	100	10	67.3	95	30	29.6 ± 0.12	No	V-1



composites, thus prevents further degradation of the original polymer matrix, as shown in Fig. 3b.

The thermal degradation process of E-HK composites was evaluated by FTIR. The FTIR spectra of E-HK composites at several representative temperatures selected according to the results of TG, such as 30, 200, 300, and 400 °C, are shown in Fig. 3c. As the temperature was raised from 30 to 200 °C, there was no obvious change in the intensity of these two absorptions, which agrees with the fact that there is no notable weight loss in the TG investigation before 200 °C, reveals that these two samples are thermally stable below 200 °C. It is worth noting that the peak near 1361 cm^{-1} belongs to the C–N bond in tertiary amine,¹⁴ which indicates that HCCP–KH450 is involved in the curing reaction of epoxy resin. When the temperature is higher than 300 °C, it is found that all peaks nearly reduced, indicating that E-HK composites decompose mainly at this stage. In addition to, at 300 °C and 400 °C, the appearance of the new peak at 1238 and 1099 cm^{-1} , which is assigned to the vibration of P=O and P–O–P bond respectively, indicates the formation of thermal stable phosphate, polyphosphate (P_2O_5 and P_4O_{10}), pyrophosphoric acid, or metaphosphoric acid.^{20,23} The peaks at 939 and 803 cm^{-1} , representing the Si–O–Si bond, appear which indicates the formation of Si–O–Si char layer.^{20,26} The appearances of all these characteristic peaks reveal the process of the char layer formation.

Flame retardancy of EP and E-HK composites

LOI and UL-94 tests are used to study the flame retardancy of EP and E-HK composites. Flame retardant samples prepared according to standard dimensions (125 mm × 13 mm × 3 mm) were used in UL-94 tests. Composition, determination results of LOI and UL-94 are summarized in Table 1. The amount of curing agent in E-HK is lower than that in EP. It is because that the secondary amine group in HCCP–KH540 participates in the curing reaction of epoxy resin and acts as a curing agent, which is evidenced by FTIR in the previous section. It can be observed from Table 1 that the LOI value of EP without flame retardant is only 22.4%, and no rating is determined in the UL-94 test. After incorporating with HCCP–KH540, the LOI value of E-HK improves with the increasing addition of HCCP–KH540. However, there is still no rating in UL-94 tests until the addition amount of HCCP–KH540 was 10 phr (dosage in per hundred

grams of EP). This is due to that a large amount of N element is fixed and cannot result in a “blowing-out effect” in gaseous phase for improving the flame retardancy of E-HK composites. Incorporating the HCCP–KH540 into EP resin, the LOI value of E-HK improves evidently from 25.5 to 29.6% and obtained a V-1 rating in UL-94 tests when the amount of HCCP–KH540 is 30 phr. It results from the EP molecular chain is entangled with the branch chain on the HCCP–KH540 conjugate ring to form a network structure, which increases the viscosity of EP composites and prevents the generation of droplets, thus endowing E-HK composite high flame retardant performance. In addition, the existing phosphorus-containing functional groups, such as P–N, P–O and P=O bonds, increase the thickness and density of the EP surface protective layer and can prevent effectively oxygen from contacting with the underlying material.

To confirm the bonding form of char residues obtained by combustion of EP and E-HK-30 composites (defined as CR-EP and CR-E-HK-30, respectively), the XPS spectra of char residues are measured as shown in Fig. 4a–e. The peaks centered at 280, 400, and 530 eV are assigned to the binding energies of C 1s, N 1s, and O 1s, respectively (see Fig. 4a). The peaks near 103 and 134 eV belong to the binding energies of Si 2p and P 2p, respectively. In the C 1s fitting spectrum of CR-EP and CR-E-HK-30 (see Fig. 4b and c), there are four kinds of bonding forms of C element: C–C (284.8 eV), C–N (285.6 eV), C–O (286.4 eV) and C=O (288.4 eV).^{27–30} Furthermore, the content of carbon oxide in CR-E-HK-30 (integral area of C–O and C=O characteristic peak) is much lower than that in CR-EP, which indicates that the addition of E-HK-30 makes it more difficult for EP to form carbon oxide. In the P 2p fitting spectrum of CR-EP and CR-E-HK-30 (see Fig. 4d), there are three kinds of bonding forms of P element: $\text{P}_2\text{O}_5/\text{P}_2\text{O}_7^{2-}$ (135.2 eV), PO_3^{2-} (134.1 eV), and PO_4^{3-} (133.4 eV).³¹ In Fig. 4e, the position of the Si 2p peak in CR-E-HK-30 is at 103.6 eV, which is assigned to the binding energies of Si–O/Si=O.²⁶ These results correspond well with the analysis of FTIR results in the previous section.

SEM and Raman spectra of char residues obtained by EP, E-HK-10, and E-HK-30 are shown in Fig. 5a–f. Encouragingly, it can be clearly observed from Fig. 5a–c that the thickness of char residue layer on the surface of EP and E-HK composites increases gradually as the increasing addition of HCCP–KH540. The presence of abundant P, N and Si containing functional

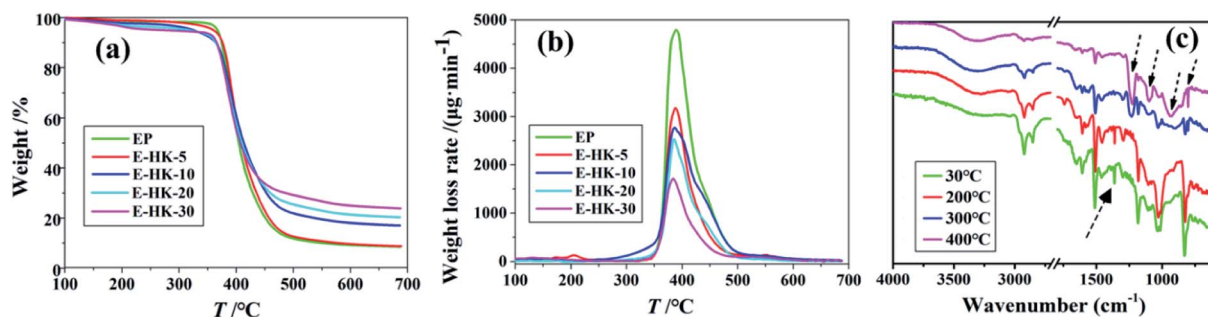


Fig. 3 Thermal stability of EP and E-HK: (a) TG curves, and (b) weight loss rate (c) FTIR spectra of E-HK composites at different temperatures.



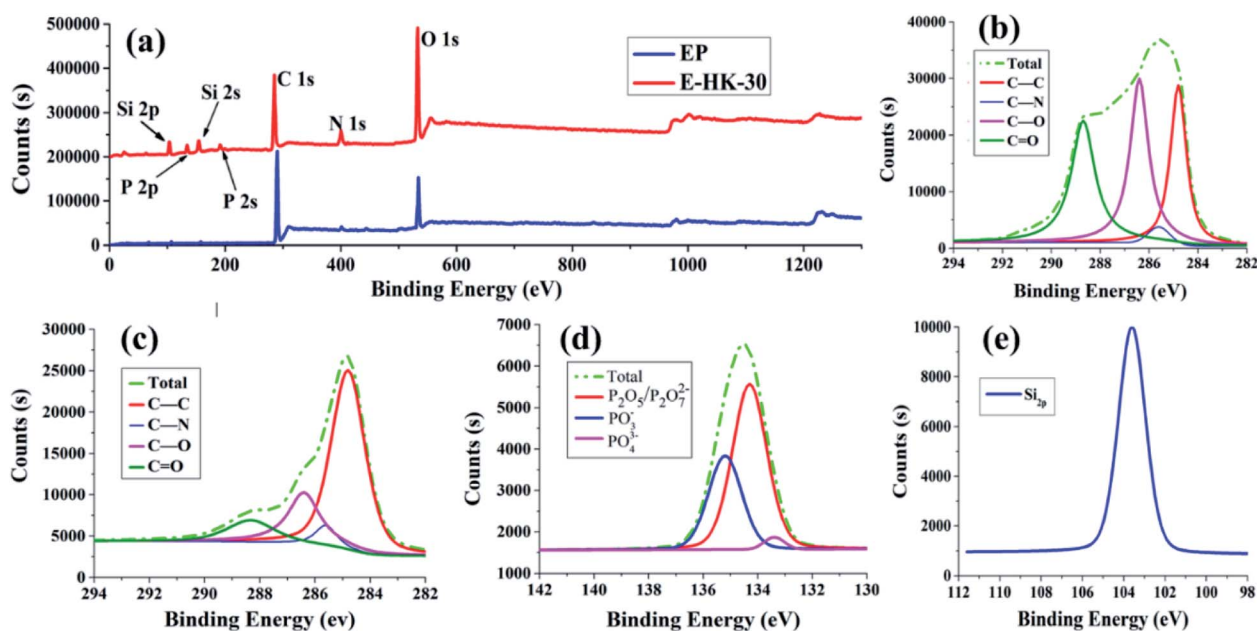


Fig. 4 Structural characterization of CR-EP and CR-E-HK-30. (a) XPS of CR-EP and CR-E-HK-30; (b) C 1s spectra of CR-EP; (c) C 1s spectra of CR-E-HK-30; (d) P 2p spectra of CR-E-HK-30; (e) Si 2p spectra of CR-E-HK-30, respectively.

groups in HCCP-KH540 can produce pyrophosphoric acid and phosphoric acid with forceful dehydration effect during combustion. Moreover, the functional groups can produce silicic acid and silicates with strong oxygen isolation effect.⁴ In particular, a large amount of residual carbon was produced after combustion, which interferes effectively with the thermal degradation process of EP composites and improves the thermal stability of EP composites. These results are confirmed by further Raman spectroscopy analysis of residual carbon, which is summarized in Fig. 5.

Raman spectroscopy analysis is an extremely important method to characterize the graphitization degree of char residues obtained by combustion of organic polymer composites. The higher the graphitization degree, the better the protective effect of the char layer. The graphitization degree of the char layer is usually expressed by I_D/I_G (the integral area ratio of peak D and G). The smaller I_D/I_G value, the higher graphitization degree of char residues and the stronger organic polymer composites ablation resistance.^{31,32} From Fig. 5d–f, the I_D/I_G value of CR-EP, CR-E-HK-10 and CR-E-HK-30 is 2.76, 2.26 and

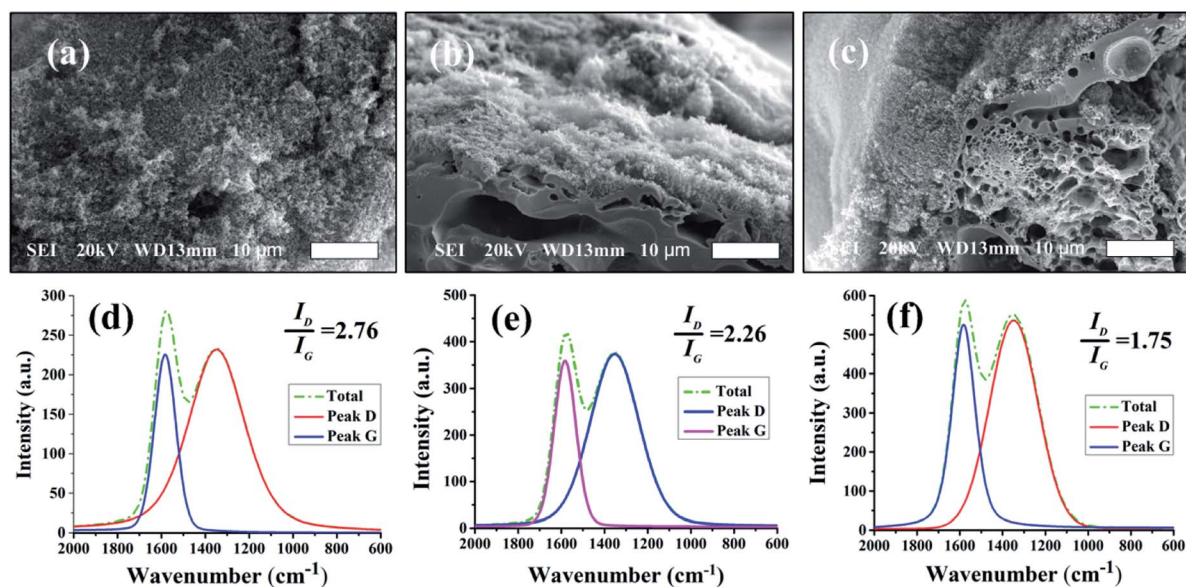


Fig. 5 SEM and Raman spectra of char residues: (a) and (d) EP, (b) and (e) E-HK-10, (c) and (f) E-HK-30.



1.75 respectively, which indicates that E-HK can improve the graphitization degree of char residues and ablation resistance of organic polymer composites.

In order to evaluate the combustion properties of EP and E-HK composites, a cone calorimeter model Icone Classic FTT was used. In this test, peak heat release rate (PHRR), time to peak heat release rate (T-PHRR), total heat release (THR), total smoke release (TSR), average CO yield (CO-Y), and average CO₂ yield (CO₂-Y) are each measured. The results are summarized in Table 2 and Fig. 6. The neat EP burns fiercely when it encounters a fire source, reaching the maximum HRR of 798 kW m⁻² quickly and releasing a great deal of heat during combustion (see Fig. 6a). But E-HK-10 and E-HK-30 present PHRR value of 617 and 494 kW m⁻², respectively. The corresponding T-PHRR increased from 28 to 40 s, which indicates that the incorporation of HCCP-KH540 can delay the combustion process and reduce the release of combustion heat. As shown in Fig. 6b, the THR of EP and E-HK composites reduced from 127 MJ m⁻² to 75 MJ m⁻². Meanwhile, both CO-Y and CO₂-Y gradually decreased with increasing HCCP-KH540 content (see Table 2). This demonstrates that HCCP-KH540 decomposed to produce PO· and terminated the free-radical chain reactions of the EP matrix. The siloxane groups tended to migrate to the surface of E-HK during combustion, at which point a compact and inorganic silica-rich layer with strong “oxygen isolation effect” was formed.

Fire growth rate (FIGRA), defined as the ratio of PHRR to T-PHRR, is used to estimate the fire hazard of materials. Lower values of FIGRA signify the improved fire safety of a given material.^{33–35} The FIGRA value of samples is summarized in Table 2. It can be observed from Table 2 that the FIGRA value reduced from 28.5 kW m⁻² s⁻¹ (EP) to 12.4 kW m⁻² s⁻¹ (E-HK-

30), which indicates that the significantly improved fire safety and fire retardancy of the EP with the HCCP-KH540.

Conclusions

Star-like molecules containing P, N and Si with dual functions of flame retardant and curing promotion (*i.e.* HCCP-KH540) were successfully synthesized through the nucleophilic substitution reaction of HCCP and KH540. The structure of HCCP-KH540 was confirmed by FT-IR, ¹H NMR and ³¹P NMR. Dynamic DSC results of EP and E-HK based on Ozawa and Kissinger methods showed that HCCP-KH540 can reduce the activation energy of curing reaction and accelerate the curing reaction rate of E-HK composites. The consequences of LOI, UL-94, cone calorimetry (CC) test and XPS, Raman, SEM analysis of char residues after combustion further showed that the flame retardant performance of E-HK is significantly improved with the addition of HCCP-KH540. The prepared composites showed great potential for application as multifunctional advanced materials in various fields, such as in electronic packaging and sealant.

Conflicts of interest

There are no conflicts to declare.

Acknowledgements

This research was funded by the National Natural Science Foundation of China (grant no. 21908086) and the Youth Science Foundation of Jiangsu University of Technology (grant no. KY19031). It was supported by Qidong NEXTER New Material Technology Co., Ltd, Jiangsu (grant no. KYH22042).

Table 2 Data from cone tests

Samples	PHRR (kW m ⁻²)	THR (MJ m ⁻²)	T-PHRR (s)	TSR (m ² m ⁻²)	CO-Y (kg kg ⁻¹)	CO ₂ -Y (kg kg ⁻¹)	FIGRA (kW m ⁻² s ⁻¹)
EP	798	127	28	24	0.032	1.6	28.5
E-HK-10	617	103	36	15	0.018	1.3	17.1
E-HK-30	494	75	40	11	0.014	1.2	12.4

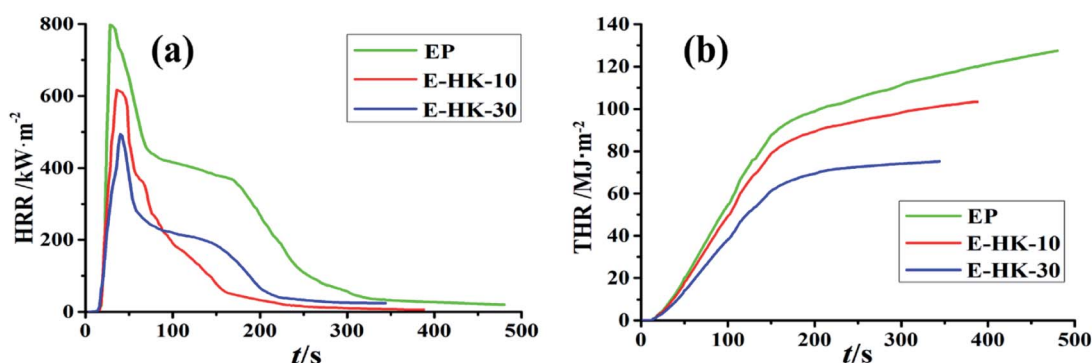


Fig. 6 HRR curves (a) and THR curves (b) for samples under an external heat flux of 50 kW m⁻².



References

- 1 A. F. Yee and R. A. Pearson, Toughening mechanisms in elastomer-modified epoxies, *J. Mater. Sci.*, 1986, **21**, 2462–2474.
- 2 Y. Ye, H. Chen, J. Wu and L. Ye, High impact strength epoxy nanocomposites with natural nanotubes, *Polymer*, 2007, **48**, 6426–6433.
- 3 Q. Y. Liu, Y. L. Zhao, S. S. Gao, *et al.*, Recent advances in the flame retardancy role of graphene and its derivatives in epoxy resin materials, *Composites, Part A*, 2021, **149**, 106539.
- 4 Z. Zhan, Y. Zhang and Y. Zhang, Improving the flame retardancy and electrical conductivity of epoxy resin composites by multifunctional phosphorus-containing polyaniline, *Mater. Lett.*, 2020, **261**, 127092.
- 5 L. Luo, F. Zhang and J. Leng, Multi-performance shape memory epoxy resins and their composites with narrow transition temperature range, *Compos. Sci. Technol.*, 2021, **213**, 108899.
- 6 L. B. Liu, Y. Xu, M. Xu, *et al.*, Economical and facile synthesis of a highly efficient flame retardant for simultaneous improvement of fire retardancy, smoke suppression and moisture resistance of epoxy resins, *Composites, Part B*, 2019, **167**, 422–433.
- 7 X. Wang, H. Yuan, S. Lei, *et al.*, Flame retardancy and thermal degradation mechanism of epoxy resin composites based on a DOPO substituted organophosphorus oligomer, *Polymer*, 2010, **51**, 2435–2445.
- 8 V. V. Petrakova, V. V. Kireev, D. V. Onuchin, *et al.*, Benzoxazine monomers and polymers based on 3,3'-Dichloro-4,4'-Diaminodiphenylmethane: Synthesis and Characterization, *Polymers*, 2021, **13**(9), 13091421.
- 9 M. Baskaran, R. Hashim, J. Y. Leong, *et al.*, Flame retardant properties of oil palm trunk particleboard with addition of epoxy resin as a binder and aluminium hydroxide and magnesium hydroxide as additives, *Bull. Chem. Soc. Jpn.*, 2019, **12**(4), 138.
- 10 Y. Fang, L. Qian and Z. Huang, Synergistic barrier flame-retardant effect of aluminium polyhexamethylenephosphinate and bisphenol-A bis(diphenyl phosphate) in epoxy resin, *Polym. Int.*, 2017, **66**(5), 719–725.
- 11 P. Wang, L. Chen, H. Xiao, *et al.*, Nitrogen/sulfur-containing DOPO based oligomer for highly efficient flame-retardant epoxy resin, *Polym. Degrad. Stab.*, 2019, **171**, 109023.
- 12 K. Rhili, S. Chergui, A. S. Eldouhaibi, *et al.*, Hexachlorocyclotriphosphazene functionalized graphene oxide as a highly efficient flame retardant, *ACS Omega*, 2021, **6**(9), 6252–6260.
- 13 O. Dagdag, M. E. Gouri, Z. S. Safi, *et al.*, Flame retardancy of an intumescent epoxy resin containing cyclotriphosphazene: experimental, computational and statistical studies, *Iran. Polym. J.*, 2021, **30**, 1169–1179.
- 14 X. Huang, F. Jing, Y. Lin, *et al.*, Synthesis of a novel cyclotriphosphazene and its enhancement of anti-aging and flame retardancy of polyolefin, *ChemistrySelect*, 2020, **5**, 9486–9491.
- 15 K. Ning, L. L. Zhou and B. Zhao, A novel aminothiazole-based cyclotriphosphazene derivate towards epoxy resins for high flame retardancy and smoke suppression, *Polym. Degrad. Stab.*, 2021, **190**, 109651.
- 16 K. Rhili, S. Chergui, A. S. Eldouhaibi and M. Sij, Hexachlorocyclotriphosphazene functionalized graphene oxide as a highly efficient flame retardant, *ACS Omega*, 2021, **6**, 6252–6260.
- 17 Z. Jiang, Q. Wang, L. Liu, *et al.*, Dual-functionalized imidazolium ionic liquids as curing agents for epoxy resins, *Ind. Eng. Chem. Res.*, 2020, **59**, 3024–3034.
- 18 X. Liu, X. Luo, B. Liu, *et al.*, Toughening epoxy resin using a liquid crystalline elastomer for versatile application, *ACS Appl. Polym. Mater.*, 2019, **1**, 2291–2301.
- 19 T. Chen and B. Liu, Enhanced dielectric properties of poly(vinylidene fluoride) composite filled with polyaniline-iron core-shell nanocomposites, *Mater. Lett.*, 2018, **210**, 165–168.
- 20 W. W. Simons, *The Sadtler Handbook of Infrared Spectra*, Philadelphia, USA, 1978.
- 21 J.-F. Kuan and K.-F. Lin, Synthesis of hexa-allylamino-cyclotriphosphazene as a reactive fire retardant for unsaturated polyesters, *J. Appl. Polym. Sci.*, 2003, **91**, 697–702.
- 22 G. R. Fulmer, A. J. M. Miller and N. H. Sherden, NMR chemical shifts of trace impurities: common laboratory solvents, organics, and gases in deuterate fulmer, *Organometallics*, 2010, **29**, 2176–2179.
- 23 Q. Wang, L. Xiong, H. Liang, *et al.*, Synthesis of a novel polysiloxane containing phosphorus, and boron and its effect on flame retardancy, mechanical, and thermal properties of epoxy resin, *Polym. Composite.*, 2016, **39**, 807–814.
- 24 H. E. Kissinger, Reaction kinetics in differential thermal analysis, *Anal. Chem.*, 1957, **29**, 1702–1706.
- 25 T. Ozawa, A new method of analyzing thermogravimetric data, *Bull. Chem. Soc. Jpn.*, 1965, **38**, 1881–1886.
- 26 W. Zhang, X. Li and R. Yang, Study on the change of silicon and phosphorus content in the condensed phase during the combustion of epoxy resin with OPS/DOPO, *Polym. Degrad. Stab.*, 2014, **99**, 298–303.
- 27 Y. Yao, M. Wang, H. Wu, *et al.*, Synthesis of waterborne epoxy resin with diethanolamine-assisted succinimide for improving the strand integrity of polyimide filament, *J. Ind. Text.*, 2021, **50**(12), 1–15.
- 28 F. Lin, W. Li, Y. Tang, *et al.*, High-performance polyimide filaments and composites Improved by O₂ plasma treatment, *Polymers*, 2018, **10**(7), 695.
- 29 K. Kiattipornpithak, N. Thajai, T. Kanthiya, *et al.*, Reaction mechanism and mechanical property improvement of poly(lactic acid) reactive blending with epoxy resin, *Polymers*, 2021, **13**(15), 2429.
- 30 Z. Yang, X. Meng, Y. Zhu, *et al.*, Single-atom platinum or ruthenium on C₄N as 2D high-performance electrocatalysts for oxygen reduction reaction, *Chem. Eng. J.*, 2021, **426**, 131347.



- 31 S. Bourbigot, M. Bras, R. Delobel, *et al.*, XPS study of an intumescent coating: II. Application to the ammonium polyphosphate/pentaerythritol/ethylene terpolymer fire retardant system with and without synergistic agent, *Appl. Surf. Sci.*, 1997, **120**(1–2), 15–29.
- 32 R. Hardis, J. Jessop, F. Peters, *et al.*, Cure kinetics characterization and monitoring of an epoxy resin using DSC, Raman spectroscopy, and DEA, *Composites, Part A*, 2013, **49**, 100–108.
- 33 S. Wang, S. Wang, M. Shen, *et al.*, Biobased phosphorus Siloxane-containing polyurethane foam with flame-retardant and smoke-suppressant performances, *ACS Sustainable Chem. Eng.*, 2021, **9**(25), 8623–8634.
- 34 S. Wang, X. Yang, Z. Li, *et al.*, Novel eco-friendly maleopimaric acid based polysiloxane flame retardant and application in rigid polyurethane foam, *Compos. Sci. Technol.*, 2020, **198**, 108272.
- 35 T. Mariappan, Z. You, J. Hao, *et al.*, Influence of oxidation state of phosphorus on the thermal and flammability of polyurea and epoxy resin, *Eur. Polym. J.*, 2013, **49**(10), 3171–3180.

